



Estimation of precipitation over Asia by combined use of gauge and multi-satellite sensor observations at fine scale

Anoop Mishra¹, A. Yatagai¹, A. Hamada¹, and R. M. Gairola

¹Research Institute for Humanity and Nature, Kyoto, Japan

²Space Applications Centre, ISRO, Ahmedabad, India

Abstract:

In the present study an effort is made to estimate the 3-hourly rainfall using gauge and satellite observations over the land and ocean region of Asia (40° S-50° N, 40° E-130° E) at 0.25° × 0.25° spatial resolution. The study utilizes the observations from rain gauge, Special Sensor Microwave/Imager (SSM/I) onboard Defense Meteorological Satellite Program (DMSP), Precipitation Radar (PR) onboard Tropical Rainfall Measuring Mission (TRMM) and geo-stationary satellite Meteosat from Eumetsat. The present study makes use of rainfall estimates by synergistic use of multi-satellite sensors using Meteosat Infrared and Water Vapor absorption channel and PR observations (Mishra et al., 2009, 2010) and SSM/I derived microwave estimates using regional scattering index developed by Mishra et al. (2009). The rain areas over the land portion of area of study is filled by available rain gauge observations over southern part (around 14° N and 78° E) of the area of the study having the dense network of Indian Space Research Organization (ISRO) Automatic Weather Station (AWS) rain gauges other parts of area of the study is filled by available microwave observations followed by the microwave calibrated infrared observations over the land and oceanic region of area of study. The precipitation estimates from the present approach is validated against rain gauge observations and other available standard rainfall products. The validation results show that present approach of precipitation estimation is able to estimate the rainfall with a very good accuracy.

Data sources:

The primary data used for this study is (1) Infrared and Water vapor observations from Meteosat, (2) microwave observations from TRMM and DMSP, which are satellites in low earth orbits. The conventional data is obtained from AWS for the validation purpose. Intercomparison of the estimates has been performed using available standard products like GPCP, and TRMM-3B42V6. The location of the ISRO AWS rain gauges is shown in figure 1.

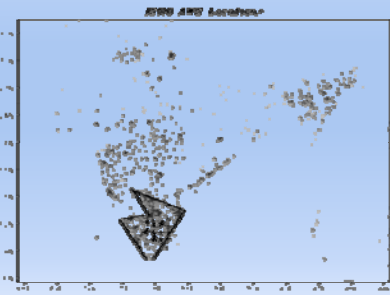


Figure 1. ISRO AWS rain gauge distribution over the Area of the study. Stations which are used for the algorithm development are shown by the black bounded box in the figure.

Methodology:

- The southern part (around 14° N and 78° E) of the area of the study is having the dense network of ISRO AWS rain gauges (shown by the bounded box in figure 1). The density of the gauges is such that at least 2-6 gauges fall within 0.25° × 0.25 over the most part of the region. From this, spatially averaged rainfall estimates were constructed using a simple spatial averaging technique. If the number of gauges is less than 2 in 0.25° × 0.25° box, then the pixels within the box are calibrated using weighted averaging by making use of the meteosat infrared brightness temperature based on the matchups between the rain from the rain gauge and the meteosat brightness temperature.

- Rainfall over the remaining part of the area of the study is estimated by the available SSM/I observations using regional scattering index technique (Mishra et al., 2009) developed separately for the land and oceanic part of the area of the study. For the development of the scattering index, the following form of relationship between 19, 22 and 85 GHz is established under non rainy conditions.

$$F=A+B*TV(19)+C*TV(22)+D*(TV(22)**2) \quad (1)$$

where F=85 GHz channel Brightness temperature.

For the land region the value of the coefficients were found as
A= 448.6809, B= -1.5456, C= -0.6020, D= 0.0055

Similarly for the oceanic regions the values of coefficients were

A= -362.4467, B= 1.1379, C= 3.5247, D= -0.0078

scattering index at 85 GHz channel is defined as

$$SI(85) = F - TV(85) \quad (2)$$

Now the SI has been calibrated with PR measurements

$$RR \text{ (mm/h)} = .0268*(SI)**1.5978 \quad (3)$$

$$RR \text{ (mm/h)} = .0118*(SI)**1.4985 \quad (4)$$

The above two equations over land and ocean are applied to get the rainfall using scattering index

- If the rain gauge and microwave observations are missing then the gap (both temporal and spatial) over the area of the study is filled by the microwave calibrated infrared observations by the application of synergistic use of multi-satellite sensor observations (Mishra et al., 2010).

This procedure begins with the cloud classification scheme following Roca et al. (2002) from meteosat IR and WV channels to identify the thin cirrus, deep convective and very deep convective clouds over 0.25° × 0.25° grid box. Finally the rainfall rates is computed based on the nonlinear power law relation between the collocated and near simultaneous IR-TBs and PR rainfall rates in 0.25° × 0.25° grid R=16.6614 × exp(-(TB-204.57)/16.52688) (5)

So the rainfall over the vacant area (where the rain gauge and microwave observations are absent) is estimated by applying the above equation using meteosat data.

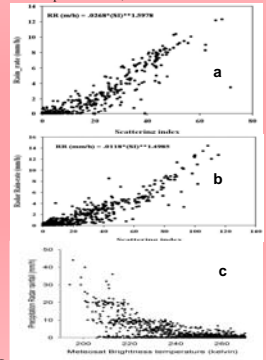


Figure 2. a) Relationship between the scattering index from the SSM/I and rainfall from PR for the land portion (b) same as fig. 2a but for the oceanic region (c) Relationship between Meteosat brightness temperature and PR-rain rates.

Comparison with TRMM-3B42V6

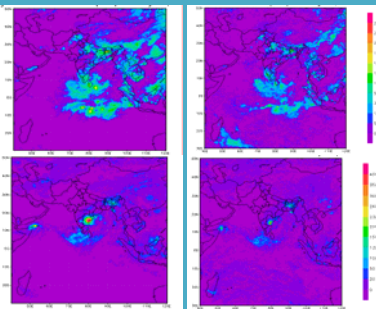


Figure 3. Daily rain (mm) over the area of study at 0.25° × 0.25° grid box (a) on 16 August, 2009 from present technique (b) on 16 August, 2009 from TRMM-3B42V6 (c) on 20 May 2010 from present technique (d) on 20 May 2010 from TRMM-3B42V6

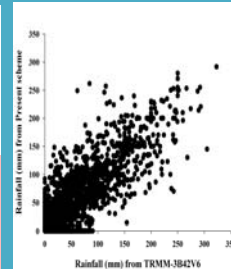


Figure 4. Scatter plot between the TRMM-3B42V6 and present scheme daily rainfall at 0.25° × 0.25° grid box

No. Of data points	61064
Correlation coefficients	0.86
Root Mean Square Error (mm)	15.28
Bias (mm)	1.12
TRMM-3B42 mean (mm)	10.68
Present scheme mean (mm)	11.80
Probability of detection (POD)	0.72
False Alarm Ratio (FAR)	0.25
Heidke Skill Score	0.23

Validation with AWS rain gauge

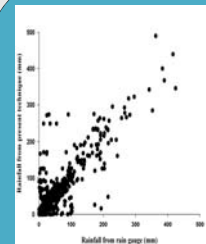


Figure 7. Scatter plot between rainfall from present scheme and rain gauge observations at 0.25° × 0.25° grid box

No. Of data points	1371
Correlation coefficients	0.77
Root Mean Square Error (mm)	27.1
Bias (mm)	4
Rain gauge mean (mm)	24.0
Present scheme mean (mm)	26.7
Probability of detection (POD)	0.83
False Alarm Ratio (FAR)	0.34
Heidke Skill Score	0.29

Comparison with GPCP V2

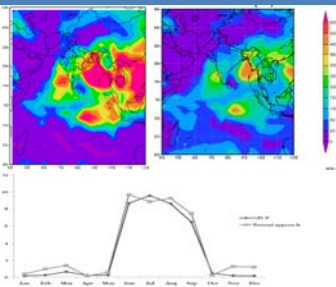


Figure 5. Monthly rain (mm) over the area of study at 2.5° × 2.5° grid box (a) on June, 2009 from present technique (b) on June, 2009 GPCP V2 (c) Time series plot of daily average (mm/day) monthly rainfall over the Central Indian region (20-25° N and 76-82° E) at 2.5° × 2.5° grid box from the present scheme and GPCP data for the year 2007

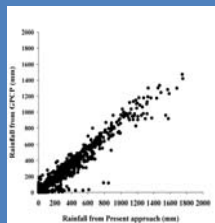


Figure 6. Scatter plot between the GPCP and present scheme monthly rainfall at 2.5° × 2.5° grid box.

No. Of data points	5024
Correlation coefficients	0.89
Root Mean Square Error (mm)	73.67
Bias (mm)	22.82
GPCP mean (mm)	151.4
Present scheme mean (mm)	174.2
Probability of detection (POD)	0.78
False Alarm Ratio (FAR)	0.19
Heidke Skill Score	0.17

Conclusions

- The present study describes the development of rainfall product for the period 2007-2010 over South Asia (30°S-50°N, 40°E-120°E) at 0.25° × 0.25° spatial resolution. The rain rates are derived by merging rain gauge and multi-sensor satellite observations.
- Validation with the rain gauges and comparison with the other satellite products shows that present approach of rainfall estimation is able to estimate the rainfall over the South Asia with a very good accuracy.
- The present rainfall product based on rain gauge, microwave observations using regional scattering index and a region specific microwave calibrated infrared observations developed for the South Asia region is able to give a very good estimates of the rainfall over the land and oceanic portion of the South Asia for the research purpose.

References

- Mishra, A., R. M. Gairola, A. K. Varma, and V. K. Agarwal, 2010, *J. Geophys. Res.*, 115, D08106, doi: 10.1029/2009JD012157.
- Mishra, A., R. M. Gairola, A. K. Varma, and V. K. Agarwal, 2009, *Curr. Sci.*, 97, 689-695.
- Mishra, A., R. M. Gairola, A. K. Varma, Sarkar Abhijit and V. K. Agarwal, 2009, *Advances in Space Res.* 44, 815-823.
- Roca, R., M. Viollier, L. Picon and M. Desbois, 2002, *J. Geophys. Res.*, 107, D19, 10.1029/2000JD000040.

Acknowledgements

This research was supported by the Environment Research and Technology Development Fund (A-0601) of the Ministry of Environment, Japan. We thank the Environmental ministry of Japan for the fund through Eco-Frontier Fellowship (A06018). We also thank MOSDAC, SAC, Ahmedabad, India for providing the AWS data. The TRMM-3B42V6, GPCP, SSM/I, and Meteosat data used in the present study are also thankfully acknowledged.